

RESEARCH ARTICLE

Locating large insects using automated VHF radio telemetry with a multi-antennae array

Kelsey Elizabeth Fisher¹  | Phil M. Dixon²  | Gang Han² | James Stephen Adelman^{3,4} | Steven P. Bradbury^{1,3}

¹Department of Entomology, Iowa State University, Ames, IA, USA

²Department of Statistics, Iowa State University, Ames, IA, USA

³Department of Natural Resources, Ecology and Management, Iowa State University, Ames, IA, USA

⁴Department of Biological Sciences, University of Memphis, Memphis, TN, USA

Correspondence

Kelsey Elizabeth Fisher
Email: kefisher@iastate.edu

Funding information

National Institute of Food and Agriculture, Grant/Award Number: Project No. IOW03617; USDA National Institute of Food and Agriculture Iowa Agriculture and Home Economics Experiment Station, Grant/Award Number: 2018-67013-27541

Handling Editor: Edward Codling

Abstract

1. We describe an automated radio telemetry system (ARTS) designed for estimating the location of 0.50 g butterflies which was constructed with commercially available materials. Previously described systems were not designed to estimate fine-scale locations of large insects within approximately 200 m² study areas.
2. The ARTS consists of four receiving stations. Each receiving station has four 3-element, directional Yagi antennae (separated by 60°) connected to an automated receiver that records detected power sequentially from each antenna. To develop and evaluate the ARTS performance, four receiving stations were installed in the corners of 4 and 6.25-ha square fields with varying heights of vegetative cover. The location of a 0.22 g transmitter was estimated with a statistical method implementing both distance- and angle-power relationships. Calibrated model parameters were based on power detected from transmitters at known locations. Using independently collected data, model performance was evaluated based on estimated locations of a georeferenced stationary transmitter, a moving transmitter with a known georeferenced path and a transmitter attached to a monarch butterfly *Danaus plexippus*. Estimated locations were calculated as frequently as every 5 s, which is at least 12 times greater than the sampling frequency previously reported for tracking insects.
3. When sufficient power data were received, the median estimated locations of a transmitter attached to an investigator's hat were <16 m from the true location. The median effective radius of the 95% confidence ellipse was 18.3 m for stationary targets and 15.9 m for a moving transmitter. Greater error in location estimation was expected when the transmitter was attached to a monarch butterfly due to interference from vegetation and variability in antenna orientation and transmitter height. As such, the median distance between the estimated and true locations was 72 m. After applying a correction for the effect of vegetation, median location error was reduced by 12 m.
4. While our ARTS has likely reached the limit of current technology, the system is still a substantial methodological advancement for locating butterflies. Our efforts should provide a benchmark as technology improves.

Kelsey Elizabeth Fisher and Phil M. Dixon contributor equally.

This is an open access article under the terms of the Creative Commons Attribution License, which permits use, distribution and reproduction in any medium, provided the original work is properly cited.

© 2020 The Authors. *Methods in Ecology and Evolution* published by John Wiley & Sons Ltd on behalf of British Ecological Society

KEYWORDS

animal tracking, automated VHF radio telemetry, *Danaus plexippus*, fine scale location estimates, insect tracking, monarch butterfly, movement ecology

1 | INTRODUCTION

Understanding animal movement across varying spatial and temporal scales is an active area of fundamental ecological research, with practical applications in the fields of conservation biology and natural resource management (Chan et al., 2019; Kays et al., 2015; Kissling et al., 2014; Nandintsetseg et al., 2019; Tobias & Pigot, 2019; Wittemyer et al., 2019). Such knowledge can support elucidation of migration patterns, home ranges, and responses to global and regional fluctuations in environmental conditions. Technology advances provide extensive potential for tracking vertebrates (ARGOS System, 2020; Hallworth & Marra, 2016; Lotek Wireless Inc., 2020; McMahon et al., 2017; Telemetry Solutions, 2017); however, options to study the movement ecology of insects are limited.

Historically, and most commonly, insect movement has been studied through visual observation. Observations, with aid of binoculars, recording theodolites, Geospatial Positioning System (GPS) units and/or compasses, allow researchers to flag and georeference locations and estimate exit angles from habitat sites when the insect can no longer be followed on foot. Researchers have employed these methods to track at least 30 butterfly species up to 50 m (Fernandez et al., 2016; Fownes & Roland, 2002; Kallioniemi et al., 2014; Merckx et al., 2003; Schultz, 1998; Schultz & Crone, 2001; Schultz et al., 2012, 2017; Skorka et al., 2013; Turchin et al., 1991; Zalucki & Kitching, 1982). Given limitations of the human visual range and associated error, potential interference of the investigator on natural behaviour of the insect and intensive effort by the researcher, visual observation provides limited means to quantify movement patterns within and between habitat patches at landscape scales. Less frequently, movement ecology of insects has been studied with the aid of tracking technologies including harmonic radar (Drake & Reynolds, 2012), very high-frequency (VHF) radio telemetry (Fisher et al., 2020; Fornoff et al., 2012; Hagen et al., 2011; Kissling et al., 2014; Levett & Walls, 2011; Liegeois et al., 2016; Svensson et al., 2011; Wang et al., 2019; Wikelski et al., 2006) and radio frequency identification (RFID; Schneider et al., 2012). The strengths and limitations of each approach depend on the behaviours of interest within relevant spatial and temporal domains (Fisher et al., 2020). The most promising technology for exploring movement, habitat use, behaviour and migration of insects is VHF radio telemetry (Kissling et al., 2014); however, applying this technology is constrained to the size of the animal. Transmitters exceeding 3% of a vertebrate animal's body weight have been shown to alter movement behaviour (Barron et al., 2010; Hallworth & Marra, 2016; Murray & Fuller, 2000). Although insects can carry transmitters up to approximately 50% of their mass (Fisher et al., 2020; Hagen et al., 2011; Liegeois et al., 2016; Srygley & Kingsolver, 2000), because of the relatively small size of insects, they require small, low-powered transmitters. For example, monarch butterflies *Danaus plexippus* weighing

approximately 0.50 g exhibit normal flight behaviour while carrying 0.30–0.25 g transmitters, which are among the smallest commercially available (Fisher et al., 2020).

Very high-frequency radio telemetry requires a receiver that detects the active transmitter signal, typically via a handheld or vehicle-mounted antenna (Kissling et al., 2014). The transmitted signal can be stored in the receiver and/or converted to an audible sound scaled to the received power. Directional antennae can be used to estimate the location of an animal without visual confirmation. If the animal is not moving, or moving slowly, the researcher can encircle the animal and determine its location based on triangulation of multiple estimated compass bearings in the direction of the most intense received signals (Lenth, 1981; White & Garrott, 1990). However, specifically when tracking insects, it is difficult, if not impossible, for one researcher to collect multiple bearings to estimate locations and reconstruct flight patterns. Alternatively, directional antennae can be used to approach an animal and facilitate visual confirmation of its true location. In the case of rapidly moving insects, researchers have followed tagged individuals on foot or in vehicles using handheld directional antennae (Hagen et al., 2011). When that approach failed, some research teams attempted to relocate transmitter signals from small aircraft, which required significant training and financial investment (Hagen et al., 2011; Wikelski et al., 2006).

Recent advancements have improved the means of using VHF radio telemetry to track insects. For example, the Motus Wildlife Tracking System is a collaborative, global automated radio-telemetry network of over 900 receiving stations designed to facilitate landscape-scale research of migratory animals (Motus Wildlife Tracking System, 2020; Taylor et al., 2017), and was used by Knight et al. (2019) to track the North American fall monarch butterfly migration. These researchers estimated that migratory monarchs traversed an average of 61 ± 42 km/day. On a landscape scale, a single researcher tracked migratory golden birdwing butterflies *Troides aeacus* across 4 km over a 4-day period using a directional, handheld antenna and a 'directional-strength' analytical technique (Wang et al., 2019). Attempts were made to detect tagged butterflies every 30 min; approximately 38% of these attempts resulted in estimated locations. These techniques provide temporally coarse estimates of insect movement and are not applicable for quantifying movement at finer scales that are still beyond human visual acuity. To fill this methodological gap, Fisher et al. (2020) stationed four researchers with directional antenna-receiver units around the release site of radio-tagged monarch butterflies and collected simultaneous bearings at 1-min interval. These bearings were subsequently triangulated to estimate locations within and immediately adjacent to a 4-ha restored prairie. This method provided the means to quantify estimated locations with associated error on a biologically relevant time-scale to recreate movement paths and estimate habitat utilization. Although successful, this method has

practical limitations, including operator fatigue during long data collection sessions, inter-operator differences in audible detection of signals, inability to estimate locations in <1-min interval and the need for additional operators to increase spatial coverage.

Automated radio telemetry systems (ARTS) have been proposed as a means to increase scalability, frequency in data collection intervals and potentially minimize errors in location estimates for insects (Kissling et al., 2014). Several research teams have described ARTS for tracking mammals and birds (Cochran et al., 1965, 2001; Crewe et al., 2019; Kays et al., 2011; Knight et al., 2019; Larkin et al., 1996; Lenske & Nocera, 2018; Motus Wildlife Tracking System, 2020; Ward et al., 2013). Most notably Kays et al. (2011) designed and utilized an ARTS to track rainforest birds and mammals on Barro Colorado Island, Panama. This system incorporated seven custom, automated receiving units on 40 m receiving stations to cover an area of roughly 1,500 ha. Each receiving station housed six, six-element directional Yagi antennae pointing in known bearing directions. The advances of Kays et al. (2011) and others to track animals ranging from 21 to 10,000 g in size provide the framework we used to develop an ARTS designed for tracking 0.5 g insects, carrying low powered transmitters, over spatial scales of 4–6 ha.

Here, we describe an ARTS that was originally designed to study movement of non-migratory monarch butterflies beyond human visual range (approximately 200 m²) on a fine temporal scale. The monarch butterfly is at risk of quasi-extinction (Semmens et al., 2016), in part, from the loss of breeding habitat in agricultural landscapes of the Midwest United States (Thogmartin et al., 2017). Because adult females are not patch-resident, egg abundance and distribution across the landscape is a function of their perceptual range, flight directionality, and flight step lengths (Grant et al., 2018; Zalucki et al., 2016). Increased understanding of female monarch movement through empirical studies in landscapes with different spatial patterns of restored breeding habitat is needed to improve predictions of realized fecundity (Fisher et al., 2020). Our ARTS was built modularly with commercially available materials to reduce costs and simplify installation at different research sites. We demonstrate successful location estimates of stationary and moving transmitters and address the influence of transmitter orientation and vegetative cover on the detection of radio-tagged monarchs and the precision of their estimated locations. We conclude with a discussion of the ARTS strengths, limitations and future research directions.

2 | MATERIALS AND METHODS

2.1 | Overview

This ARTS, designed for estimating locations of insects beyond human visual ability on a fine temporal scale, was built with commercially available materials and adapted from the system described by Kays et al. (2011). We describe our ARTS design and statistical model, including:

1. Transmitter, antennae, receivers and design to collect multiple measurements of signal strength.
2. Statistical method development and evaluation to estimate location from the strength of the received signal.

Our ARTS consisted of four receiving stations installed and georeferenced (Trimble Geo7x) in the corners of a square grid. Each receiving station had an automated receiver and four directional antennae pointing in different directions. We used three-element Yagi antennae, rather than six-element (Kays et al., 2011), because they are lighter, which increased receiving station stability. Because we used different materials and antennae arrays, the mathematical model used by Kays et al. (2011), which incorporated a relationship between received power and angle, was not appropriate to estimate transmitter locations with our system. Our ARTS utilized a model that incorporated both power-distance and power-angle relationships. Performance of the ARTS was evaluated using a low-powered, 0.22 g transmitter, taking into account factors including height and orientation of the transmitter, vegetation between the transmitter and the receiving station, and rate and pattern of transmitter movement (see Crewe et al., 2019; Kays et al., 2011; Lenske & Nocera, 2018; Ward et al., 2013).

2.2 | System design

Receiving stations were created from 7 m tall aluminium telescoping banner stands (Figure 1a; 23 foot Mondo Outdoor Flag, San Diego Sign Company), which were stabilized with a guy wire system (EZ-GW-KIT, Solid Signal) that was augured (auger anchor kit, Grainger) approximately 0.5 m into the ground. The top 1.25 m of the pole was wrapped in electrical tape to reduce potential signal interference. Four 3-element, directional Yagi antennae (calibrated for frequencies from 164.000 to 166.000 MHz; Johnson's Telemetry) were attached to the top of the pole with hose clamps and a series of RAM mounts (RAP-B-400U, RAM-B-201U, RAM-B-231Z-2NUBU; RAM Mounts). Mounts were separated by 0.3 m, with the top mount 0.9 m higher than the bottom mount. The claw clamp of the mount (RAP-B-400U) was attached between the middle and bottom parallel elements of a Yagi antenna, which held the antenna in the vertical orientation (Figure 1b). A vertical orientation was used to maximize detection of transmitter signals with increasing distance from a receiving station, rather than a horizontal orientation that has greater ability to discern directionality, but with a lower limit of detection with distance (Cochran et al., 1965, 2001; Larkin et al., 1996). Yagi antennae were positioned 60 apart, so the top and bottom antennae were pointed 180 from each other. The space between the middle two Yagi antennae pointed towards the centre of the field. To obtain the true direction of the Yagi antennae, compass bearings were taken while standing behind each antenna.

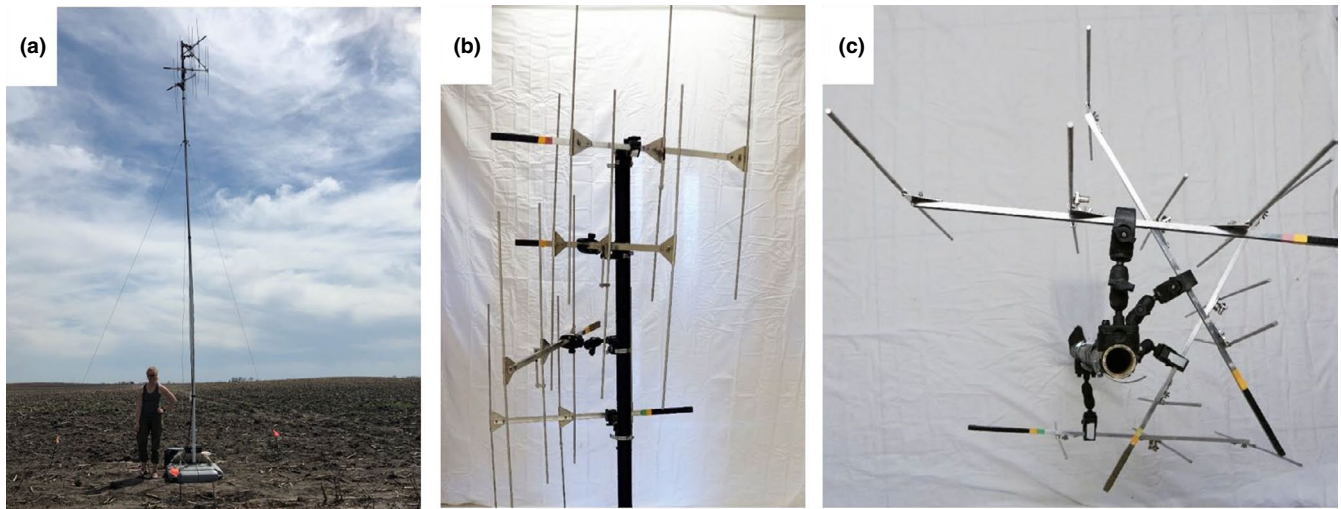


FIGURE 1 Each receiving station in our automated telemetry system consisted of four 3-element Yagi antennae attached to the top of a 7 m pole, supported by a guy wire system that was augured 0.5 m into the ground (a). Yagi antennae were placed in vertical polarization (b) separated by 60 around the pole's axis (c)

Yagi antennae were connected with 7.62 m coax cables (Lotek Wireless) to an automated receiving unit (SRX800-D, Lotek Wireless) at the base of the pole. Receivers were programmed to scan for a single, specific transmitter frequency and collect data from each Yagi antenna for 6 s; one full scan through all four antennae occurred every 24 s (Table ST1 lists the receiver programming parameters). The power of a detected transmitter was reported in Received Signal Strength Indicator (RSSI) units that are logarithmically scaled, analogous to decibels and stored in the receiver. Based on results from a preliminary evaluation of the antenna's signal detection sensitivity and directionality (Figure S1), receiver gain was set to 65, which minimized detection of signal behind the antenna.

We used LB-2X transmitters (HoloHil Systems, Ltd.), which are among the smallest available commercially (0.22 g), have approximately 8 days of battery life and have been used successfully on monarch butterflies (Fisher et al., 2020). Data that aided in development and evaluation of the statistical model to predict transmitter location were collected with the transmitter attached to a stationary investigator, a mobile investigator and a radio-tagged butterfly. After noting that LB-2X transmitters emit signal with a directional pattern when held in horizontal orientation (Figure S2), we ensured the transmitter antenna was maintained in a vertical orientation, which removed the directional pattern. When worn by an investigator, the transmitter was placed in 15 ml conical tube (Fisher Scientific) and vertically affixed to a baseball cap. When attached to the ventral side of the butterfly's abdomen with superglue (Fisher et al., 2020), the transmitter antenna was bent at a 90 angle approximately 5 mm after the end of the monarch's abdomen to maintain vertical orientation. Transmitters with a 90 bend of the antenna to the vertical orientation behaved similar to transmitters attached to the cap in vertical orientation (Figure S2). Locations of hat and stationary monarch-affixed transmitters were georeferenced (Trimble Geo7x) and adjusted

with the closest base station; after correction, error ranged from 0 to 50 mm.

2.3 | Conceptual model to estimate transmitter location

Telemetry systems can estimate location through two, non-exclusive, basic principles: (a) the strength of a received signal decreases as distance from the source increases and (b) the strength of a received signal decreases as the direction to the source deviates from the antenna's boresight angle. Traditional direction-based triangulation requires finding only the antenna angle resulting in the greatest signal strength. We devised a method to estimate location implementing both angle and distance.

Antenna physics implies that distance effects and angle effects are additive when power is measured on a logarithmic scale, like decibels or RSSI units (Balanis, 2016). The model for power, P , at an arbitrary distance, d , and angle from the antenna to the transmitter, θ , are then:

$$P = \beta_0 + f_{\text{distance}}(d) + f_{\text{angle}}(\theta). \quad (1)$$

The intercept, distance function and angle function can be estimated by recording power at a range of distance and angles. Figure S3 shows the locations to calibrate Equation (1) for one of our data collection periods.

An unknown transmitter location, (x, y) , can be estimated from contemporaneous measurements of power at multiple antennae on the same receiving station. Implementing an estimator requires specifying the form of $f_{\text{distance}}(d)$ and $f_{\text{angle}}(\theta)$, estimating any unknown parameters in those functions, and devising an estimator of the location. Details of each of these steps are provided in the following subsections.

2.3.1 | Determining $f_{\text{distance}}(d)$

According to Friis's (1946) law, the power of a received signal, measured in decibels, decreases linearly with log-transformed distance to the source. In practice, there is random variation in the received power, resulting in the model.

$$P^* = k_1 + k_2 \log(d) + \varepsilon, \quad (2)$$

where P^* is the power, d is the distance between the antenna and the transmitter and ε is the random variation.

Automated receivers have a limit of detection for radio signals. Only radio signals with power above the detection limit are recorded; signals below that limit are ignored. Hence, the recorded power has a distribution that is truncated at the detection limit. When the random variation in power follows a normal distribution, the recorded power follows a truncated normal distribution. The expected recorded power is then

$$P = P^* + \sigma \phi\left(\frac{c - P^*}{\sigma}\right) / \left[1 - \Phi\left(\frac{c - P^*}{\sigma}\right)\right], \quad (3)$$

where P is the mean recorded power, P^* is the mean power given by Equation (2), c is the receiver detection limit, σ is the standard deviation of power values, $\phi()$ is the standard normal probability density function and $\Phi()$ is the standard normal cumulative probability density function. The second term in Equation (3) is the shift in mean recorded power due to receiver failure to record below the detection limit. That shift is generally small unless the power predicted by Friis's law is close to or below the detection limit.

To confirm the theoretical relationship between distance and power given by f_{distance} , Equations (2) and (3), we collected data at a range of distances from a receiving station. We installed two receiving stations 400 m apart in a 4-ha, flat, open, harvested maize field with low to no vegetation to prevent interactions between the radio signals and the environment (Goldman & Swenson, 1999). Each receiving station had an antenna pointing directly towards the other receiving station. An investigator, wearing the transmitter, walked along a straight line between the two receiving stations four times,

stopping for 2 min every 25 m (Figure S3). Because the receiver sampled the antenna every 24 s, there were up to four instantaneous power readings per receiving station/antenna at each location. Preliminary investigation indicated that a small fraction of power readings were abnormally low over a 2-min sampling period; therefore, the median power of the 2-min interval was used to summarize the power for each of the four visits to each location. Distance from the transmitter to each receiving station was calculated assuming all antennae were 7 m above-ground. The difference between a transmitter's distance to the receiving station base and its distance to the antennae is <0.5 m at 50 m or more from the receiving station and <1 m at 25 m.

The relationship between power and log distance is linear between 25 m and approximately 140 m (Figure 2, left panel). Closer than 25 m, signals saturated the receiver. In this field setting, the receiver detection limit was about 58 RSSI units. The truncated power model, Equation (3), reasonably describes the observed power from 25 to 200 m. That fitted model is essentially identical to the linear model up to distances of c. 125 m, then asymptotes at the receiver detection limit.

2.3.2 | Determining f_{angle}

When the receiving antenna is directional, the power of a received signal also depends on the angle between the transmitter and the antenna boresight. The specific relationship depends on the antenna design. For commonly used Yagi antennas, the relationship between angle and power depends on orientation of the antenna and the number, size and spacing of parallel elements (Kuechle & Kuechle, 2012). The specific relationship requires specialized software to determine. Some antenna manufacturers provide this information, but ours did not. We digitized the radiation pattern (Figure S4) for a three-element Yagi antenna with dimensions identical to ours (Yagi-Uda.com, 2008). For angles up to 80 (≈ 1.4 radians) from the antenna boresight, the power is well approximated by $P = \alpha_0 + \alpha_1 (1 - \cos\theta)^{0.95}$. The pattern of the 'back lobe', for angles between 90 and 270, is more complex. At least part of that theoretical pattern can be approximated by $P = \alpha_2 + \alpha_3 (1 + \cos\theta)^{0.95}$. The front- and back-lobe curves can be described by a single model by

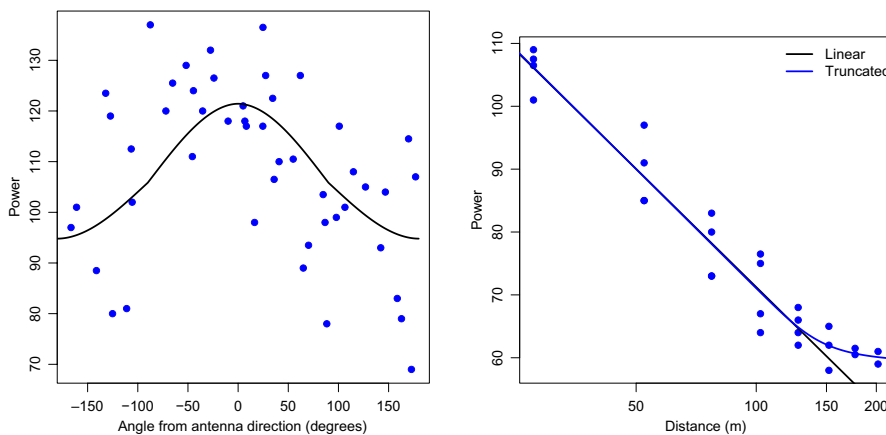


FIGURE 2 We found a clear relationship between received power and the distance between transmitter and antenna (left panel), and a more variable relationship between received power and the angle between antenna and transmitter (right panel). Panels show representative plots from a single antenna with distance on a logarithmic scale

forcing the two parts to be continuous at 90 and -90. That model for data at a constant distance is

$$P = \begin{cases} \alpha_0 + \alpha_1 [(1 - \cos\theta)^{0.95} - 1] & -90^\circ \leq \theta \leq 90^\circ \\ \alpha_0 + \alpha_2 [(1 + \cos\theta)^{0.95} - 1] & 90^\circ \leq \theta \leq 270^\circ \end{cases} \quad (4)$$

To confirm this relationship in a field setting, we installed four receiving stations in the corners of a harvested maize field with four antennae pointed at -60°, 0°, 60° and 120°. An investigator walked in a semi-circle 25 m from each receiving station base and stopped at 13 evenly distributed locations for 2-min intervals (Figure S3). This provided power readings at a variety of angles from the four antennae boresights, but at a constant distance. The theoretical pattern was fit by a segmented regression joined at 90 and -90 to account for the different curves in the front and back lobes (Figure 2, right panel). The fitted angle model for these antennae is

$$P = \begin{cases} 121.8 - 8.73 [(1 - \cos\theta)^{0.95} - 1] & -90^\circ \leq \theta \leq 90^\circ \\ 121.8 + 22.48 [(1 + \cos\theta)^{0.95} - 1] & 90^\circ \leq \theta \leq 270^\circ \end{cases} \quad (5)$$

The large random variation in power means that the bearing with the strongest signal may be quite different from the true bearing (Figure 2, right panel). Therefore, estimating location from only bearing angles does not work as well in our system as it has in others (see Kays et al., 2011).

2.3.3 | Random effects of receiving stations and antennae

Evaluation of the residuals from the fitted regression supported the assumption that the random variation in received power could be approximated by a normal distribution with constant variance. With the details of f_{distance} and f_{angle} , Equation (1) becomes

$$\mu^* = \beta_0 + \beta_1 \log(d), \quad (6)$$

$$z^* = \frac{c - \mu^*}{\sigma}, \quad (7)$$

$$\mu = \mu^* + \sigma \frac{\phi(z^*)}{1 - \Phi(z^*)} + \begin{cases} \beta_2 [(1 - \cos\theta)^{0.95} - 1] & -90^\circ \leq \theta \leq 90^\circ \\ \beta_3 [(1 + \cos\theta)^{0.95} - 1] & 90^\circ \leq \theta \leq 270^\circ \end{cases} \quad (8)$$

$$P = \mu + \epsilon, \epsilon \sim N(0, \sigma^2). \quad (9)$$

In the above equations, μ^* is the mean power before adjusting for truncation or angle effects, μ is the mean power at distance d and angle θ , and P is the observed power.

Inspection of the power readings from up to four antennae on each of up to four receiving stations suggested repeatable effects

of individual antennae. In particular, we noted antenna-specific variation in β_0 , β_2 and β_3 . If these random effects are ignored, the errors associated with each observation are not independent. We assessed these effects by fitting a mixed model generalization of Equation (12) that allowed β_0 , β_2 and β_3 to randomly vary by antenna.

$$\mu^* | \alpha_{0i} = (\beta_0 + \alpha_{0i}) + \beta_1 \log(d), \quad (10)$$

$$z^* = \frac{c - P^*}{\sigma}, \quad (11)$$

$$\mu | \alpha_{0i}, \alpha_{2i}, \alpha_{3i} = \mu^* + \sigma \frac{\phi(z^*)}{1 - \Phi(z^*)} + \begin{cases} (\beta_2 + \alpha_{2i}) [(1 - \cos\theta)^{0.95} - 1] & -90^\circ \leq \theta \leq 90^\circ \\ (\beta_3 + \alpha_{3i}) [(1 + \cos\theta)^{0.95} - 1] & 90^\circ \leq \theta \leq 270^\circ \end{cases} \quad (12)$$

$$P = \mu | \alpha_{0i}, \alpha_{2i}, \alpha_{3i} + \epsilon, \epsilon \sim N(0, \sigma^2). \quad (13)$$

When this model (Equations 12 and 13) was fit to distance and angle data from a harvested maize field, the estimated variance components for α_{0i} , α_{2i} and α_{3i} were 51, 145 and 57, while the estimated residual variance was 159. Only the data from distances between 25 and 140 m were used in the fit to essentially eliminate the consequences of truncation. Evaluation of other possible random effects indicated no evidence of an antenna effect on β_1 , the slope for $\log(\text{distance})$, or a receiving station effect on β_0 , the overall intercept.

2.3.4 | Estimating location

Consider a transmitter at an unknown location (x, y) and an antenna j pointing in direction ω_{ij} at height h on receiving station i located at (e_i, n_i) , the distance, d_{ij} , from the transmitter to the antenna is

$$d_{ij}(x, y) = \sqrt{(x - e_i)^2 + (y - n_i)^2 + h^2}, \quad (14)$$

and the angle between the antenna direction and the transmitter location, θ_{ij} , is

$$\theta_{ij}(x, y) = \tan^{-1} \left(\frac{y - n_i}{x - e_i} \right) - \omega_{ij}, \quad (15)$$

where the arc tangent function is one that correctly identifies the appropriate quadrant, for example, $\text{atan2}()$ in R (R Core Team, 2019). The expected power observed at antenna j on receiving station i from a transmitter at location (x, y) is given by Equation (12) evaluated using $d = d_{ij}$, θ_{ij} , estimated regression coefficients, β_0 , β_1 , β_2 and β_3 and the best linear unbiased predictors (BLUPs) of the random effects, α_{0i} , α_{2i} and α_{3i} .

The regression coefficients and random effects in Equation (12) are predicted by fitting a calibration dataset with known locations. We found it necessary to collect calibration data for each new field

and set of receiving station locations. Results reported here are based on calibrations using 50–75 locations per study field. The calibration locations included many collected in 25 m radius circles around each receiving station (angle calibrations), some at varying distance from one or two receiving stations (distance calibrations) and some at random locations.

When the errors, ε_{ij} associated with each observation satisfy the assumptions of independence, a normal distribution, and equal variance, the unknown location can be estimated by nonlinear least squares, or equivalently maximum likelihood. This was implemented using the `optim()` function in R (R Core Team, 2019). For most datasets, we found minimization of the error sum-of-squares to be more numerically robust than maximization of the log likelihood.

The estimated variance-covariance matrix $\hat{\Sigma}$ for the estimated location, $l = (\hat{x}, \hat{y})$, is given by the negative inverse of the Hessian matrix of the log-likelihood function evaluated at the estimated location. Equivalently, when the location is estimated by minimizing the error sum-of-squares,

$$\hat{\Sigma} = 2 \sigma^2 H^{-1}, \quad (16)$$

where H is the Hessian matrix of second derivatives of the sum-of-squares with respect to the two location coordinates, x and y .

A bivariate $1 - \alpha$ confidence region can be computed using a normal approximation (Johnson & Wichern, 2002, p. 221, with S/n replaced by $\hat{\Sigma}$). For two parameters, x and y , the confidence region boundary is the set of locations $l = (x, y)$ that satisfy

$$(l - l) \hat{\Sigma}^{-1} (l - l) = 2(n - 1) F_{1-\alpha}(2, n - 2) / (n - 2). \quad (17)$$

Alternatively, the confidence region could be computed using profile sum-of-squares (Bates & Watts, 2007).

The overall uncertainty in the location can be summarized by the effective radius of the 95% confidence interval:

$$\left(2 F_{1-\alpha}(2, n - 2) \right)^{0.25} \left| \hat{\Sigma} \right|. \quad (18)$$

When the confidence interval for the location is circular, this value is the radius of that confidence interval circle. When the confidence interval is elliptical, this value is radius of a circle with the same area as the confidence ellipse.

2.4 | Evaluating the method

2.4.1 | Estimating location of stationary transmitter at random locations

At Blue Grass Enterprises sod farm in Linn County, IA, four receiving stations were installed 250 m apart in the four corners of an approximately 6.25 ha, flat, open area. An investigator, with the

transmitter attached to the hat, stood at 62 randomly or deliberately chosen, georeferenced locations for 2-min intervals. Data from 52 strategically chosen locations were used to calibrate the model, which was then used to estimate the locations of the remaining 10 points.

2.4.2 | Estimating locations of a moving transmitter

To imitate monarch butterfly flight, while having control over speed and path, an investigator walked a straight line through the 250 m² detection area at a flat, open, harvested maize field in Story County, IA, at a pace of approximately 50 m/min for approximately 7 min. Known locations along the straight line path were georeferenced. Because the receiver only records one antenna at a time, synchronous power readings for the four antennae at a receiving station were obtained by smoothing the power versus time curve for each antenna (Figure S5). The power versus time curves were smoothed by fitting a generalized additive model with a thin-plate regression spline using `gam()` in the R `mgcv` library (Wood, 2003, 2011). Default parameters were used except for setting `gamma = 2` to obtain smoother fits. Predicted power for all antennae was calculated every 5 s, except when there was a gap of over 60 s, which corresponded to two consecutive cycles without a recorded power.

2.4.3 | Estimating locations of a mobile butterfly

Four receiving stations were installed to create a 250 m² detection area in a restored prairie with habitat in Floyd County, IA, comprised of native grasses and forbs of approximately 1.0 m in height. A radio-tagged monarch butterfly was released on a non-blooming forb and observed for 40 min by an investigator stationed 5 m away to record the nature and elapsed time of behaviours. When the butterfly was stationary, the location was georeferenced and the true time spent at that location was recorded. Likewise, the true time spent flying between stationary locations was recorded. Periods of low-level variation in received power and periods of erratic changes in received power were associated with periods when the monarch was stationary or flying, respectively. Time sequences of power received during the observation period were smoothed using a `gam()` model, as described in Section 2.4.2. Because the vegetation present in the prairie restoration was expected to lower confidence in estimated location in comparison to the sod and harvested maize fields (Crewe et al., 2019; Goldman & Swenson, 1999; Kays et al., 2011; Larkin et al., 1996), we conducted a calibration test to quantify the distance–power relationship with the transmitter placed in a potted plant (*Chrysanthemum* sp.; Figure S6). The resulting relationship paralleled that observed in the open field, but was dampened by 22 RSSI. Locations in the restored prairie were estimated every 30 s with and without employing the 22 RSSI adjustment to evaluate the extent to which the 'vegetation correction factor' improved estimates.

3 | RESULTS

3.1 | Estimating location of stationary transmitters at random locations

Locations and 95% confidence ellipses were estimated for all 10 test locations (Figure 3). Six of the transmitter's actual locations were located inside the 95% confidence ellipse for the estimated location. The other four estimated locations were outside of the 95% confidence ellipse, but were within 49.2 m of the actual location. The median distance between the estimated and actual locations was 14.7 m; the median effective radius of the confidence ellipses was 18.3 m.

When a transmitter was within 25 m of a single receiving station, the received power saturated the receiver, which limited the precision of location estimates in these situations. Similarly, if a transmitter was located outside the upper limit of the linear distance–power relationship (c. 150 m for the system in this study), recorded power readings were less reliable for estimating location because the power versus distance curve asymptotes.

3.2 | Estimating locations of a moving transmitter

Using the smoothing calculation, sequential locations were estimated using the predicted power (Figure 4) of a transmitter that

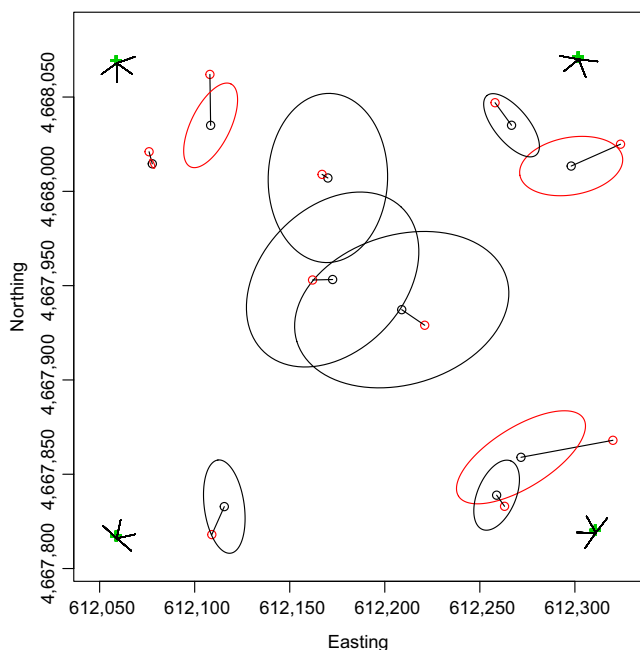


FIGURE 3 The system accurately estimated locations of 6 of the 10 test locations of stationary transmitters on a sod field at Blue Grass Enterprises. Receiving station locations are shown by green cross; short black lines away from the green cross indicate the direction of each antenna. True locations are shown in red and estimated locations are shown in black. The 95% confidence ellipses are shown in black when they include the true location and red if the estimated location does not fall within the ellipse

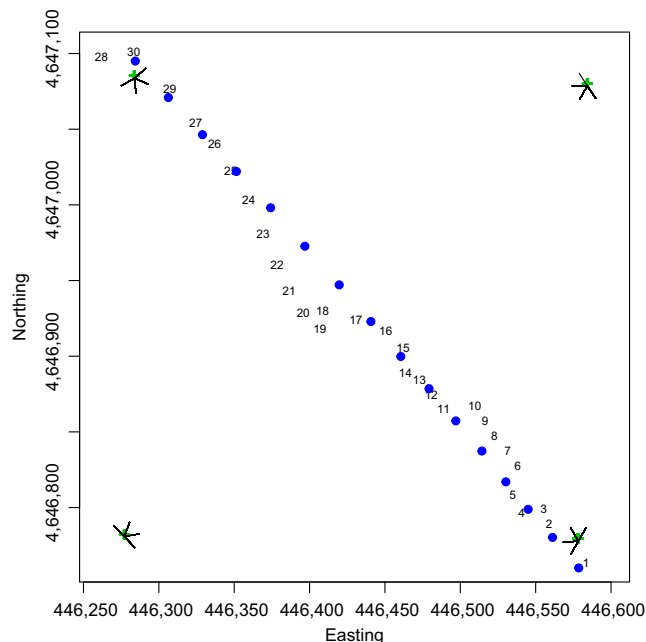


FIGURE 4 The system accurately captured the path of an investigator walking from the southeast to northwest receiving station at a pace of 50 m/min at a harvested maize field. We estimated locations every 5 s, depicted here as numerals in chronological order. Blue dots mark the investigator's georeferenced locations along the path. Receiving station locations are shown by green crosses; short black lines away from the green cross indicate the direction of each antenna

moved at a rate of approximately 50 m/min. Although not shown, 93% of the estimated locations occurred within the 95% confidence ellipse and half of the estimated locations were within 15.9 m of the actual location. All estimated locations of a moving transmitter were between 5.0 and 47.9 m from the true location. When the transmitter was within 25 m of a receiving station, estimated locations were not always consistent with actual, sequential locations. With increasing distance from receiving stations, the sequence of estimated and actual locations was concordant. Inconsistency between actual and estimated locations near receiving stations likely reflects the received power saturating the receivers.

Although location could be estimated from as few as three power readings, there was uncertainty in such estimates. When the confidence interval, Equation (17), was estimated from the three power values, the $F_{2,1}(0.95)$ quantile was 200. With four readings, the F quantile was much smaller: $F_{2,2}(0.95) = 19.0$. For example, the median sample size for the locations collected with the moving transmitter was 8, with a range from 3 to 11. Our experience suggests aiming to have at least six power readings from three receiving stations.

3.3 | Estimating location of mobile butterfly

Within the 40-min observation period, the radio-tagged monarch flew for a maximum of 20 s among four stationary locations a maximum of 44 m apart within the 250 m² detection area of the restored

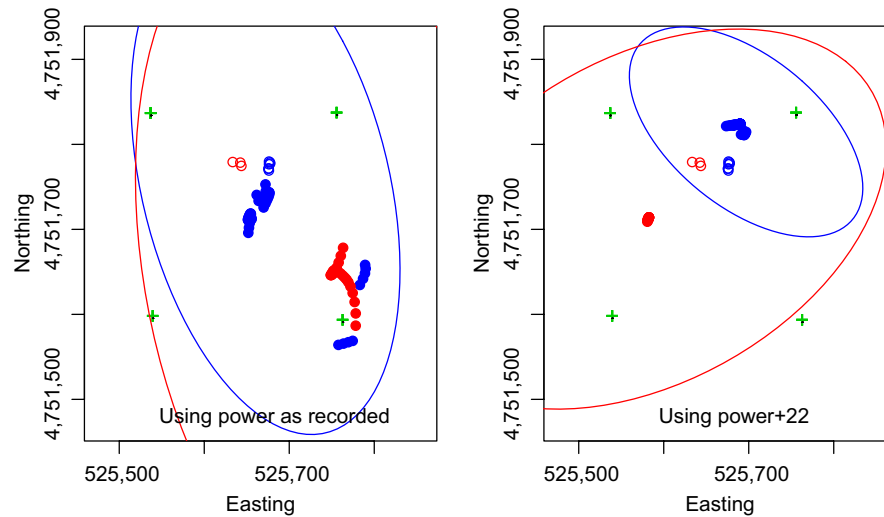


FIGURE 5 We used the ARTS to estimate locations of a radio-tagged monarch butterfly that flew for a maximum of 20 s between known stationary points associated with distinct patches of vegetation that were a maximum of 44 m apart (red vs. blue open circles; left panel). Raw RSSI signals detected by the receiving stations yielded clusters of estimated locations (filled circles) that corresponded to the known stationary points (open circles). These estimated locations were a median distance of 58 m from the butterfly's associated known locations. To offset the effect of vegetation on received signal strength, we added 22 RSSI to each of the raw values (see Section 2.4.3 Estimating locations of a mobile butterfly), which yielded estimated points that were a median of 46 m from the true locations (right panel). Representative confidence ellipses are shown for one estimated point within each cluster. Green crosses represent locations of receiving stations

prairie. The power received by the receiving stations was stable and consistent when the monarch was stationary. Variability in power was observed during times of known flight (Figure S7). All the raw data detected by the receiving stations were used to estimate 79 locations every 30 s. Consequently, we assume estimated locations are associated with the monarch stationary in the vegetation, since it is extremely unlikely a location could be estimated during the short time the monarch was in flight. Estimated locations were a median of 72 m from the true stationary locations. Confidence ellipses could not be calculated for all estimated locations because of numerical difficulties estimating the variance–covariance matrix. Two typical confidence ellipses, shown in Figure 5, had effective radii of 209 and 310 m. Error estimates were large because each location was estimated with only five or six recorded power readings and those readings were variable. To account for dampened signals due to the presence of vegetation, we added 22 RSSI to each of the raw values (see Section 2.4.3 Estimating locations of a mobile butterfly), which improved our location estimates. The 79 estimated locations based on the 22 RSSI adjustment were a median of 46 m from their associated true locations. The effective radii of the confidence intervals shown in Figure 5 were 120 and 240 m. Although the difference between actual and estimated locations ranged from 38 to 93 m, the pattern of estimated locations was concordant with the true locations between flights.

4 | DISCUSSION

Because of their relatively small size, techniques for tracking and quantifying insect movement are limited. To date, most methods are labour-intensive, rely on visual observation or collect data on

coarse time-scales. We devised an automated VHF radio telemetry system to estimate locations of insects with low-powered transmitters at a fine temporal scale beyond human visual acuity. Although additional research and future technological advances could improve error estimates, our system provides a substantial advancement in comparison to previous methods to locate butterflies. Implementation of the ARTS described here increases detection range to approximately 150 m, which exceeds a 50 m tracking limit based on visual observations (Fernandez et al., 2016; Fownes & Roland, 2002; Kallioniemi et al., 2014; Merckx et al., 2003; Schultz, 1998; Schultz & Crone, 2001; Schultz et al., 2012, 2017; Skorka et al., 2013; Turchin et al., 1991; Zalucki & Kitching, 1982), and provides the means to estimate location errors. Our system is not intended to replace traditional handheld or vehicle-mounted radio telemetry methods, but rather augment methods and alleviate personnel requirements as compared to following insects by foot or vehicle; therefore, the ARTS also provides practical advantages as compared to personnel following insects on foot with handheld radio telemetry (Fisher et al., 2020; Fornoff et al., 2012; Hagen et al., 2011; Kissling et al., 2014; Levett & Walls, 2011; Liegeois et al., 2016; Svensson et al., 2011; Wang et al., 2019; Wikelski et al., 2006).

Our statistical method to estimate location incorporated both the effect of distance and angle on the received power by each of four Yagi antennae on a receiving station, which was not explored previously (Cochran et al., 1965, 2001; Kays et al., 2011; Larkin et al., 1996). With this method, we were able to successfully estimate locations of stationary transmitters at distances beyond visual detection with a median accuracy of 14.7 m. This accuracy from a distance of up to 150 m from a receiving station

is appropriate for the spatial scale of our movement questions and is a significant improvement compared to visual observations at distances up to, but not exceeding, 50 m with no error estimates. In addition, our method produced comparable accuracy when locating a mobile transmitter attached to an investigator's hat at a temporal resolution that is 12 times more frequent than the shortest telemetry data collection interval previously reported with insects (Fisher et al., 2020; Hagen et al., 2011; Kissling et al., 2014; Knight et al., 2019; Wang et al., 2019). These results suggest under optimized conditions, with the transmitter antenna consistently vertical and 1.6 m above the ground, our system and method of estimating location can be used to reasonably quantify locations and error estimates of stationary and moving low-mass transmitters at distances beyond human vision.

When the transmitter was attached to a mobile monarch butterfly, increased error in location estimates were expected due to interference of vegetation, variability in transmitter antenna orientation when in flight and height of the transmitter (Crewe et al., 2019; Kays et al., 2011; Ward et al., 2013). Estimated locations were a median of 58 m from their associated stationary location. To compensate for decreased received power, we added an empirically derived constant 22 RSSI factor to each receiving station, which improved our location estimates and decreased the associated error. Estimated locations with the correction ranged in accuracy from 38 to 93 m and the pattern of estimated and actual locations were concordant. This approach assumes a constant vegetative effect; however, the impact of vegetation likely varies with plant height and density (Crewe et al., 2019; Kays et al., 2011; Ward et al., 2013). Further investigation could ascertain the need to use site-specific vegetation to implement appropriate corrections for interference. Representative confidence ellipses had effective radii of 120 and 240 m (see Figure 5 right panel) because locations were estimated from five or six detected power values, which impacts the multiplier that scales the variance-covariance matrix into a bivariate confidence ellipse. For example, for $N = 5$, the multiplier is 5.04 and for $N = 6$, the multiplier is 4.17. With larger sample sizes, the multiplier is considerably smaller, for example, 3.17 for $N = 10$. Although location can be estimated from relatively few detected power values, large confidence ellipses are expected.

We confirmed that periods of stable received power occurred when the monarch was stationary and periods of variability in signal strength detection were associated with flight. While we can detect when a monarch is in flight, it may prove difficult to predict location during flight because of the thin-plate regression spline smoothing function applied in our estimation method (Figure S7). The thin-plate regression spline smoothing function controlled for differences in the precise time of estimates from different receiving stations, and reasonably estimated received power in our field trials. When transmitters attached to the cap were moving slowly, fluctuations in received power over short time intervals likely represented background noise, rather than true differences in location. However, if a radio transmitter was moving rapidly or erratically, fluctuations in received power could represent true differences in the location. A

smoothing function applied to such data over time would produce estimated power values that reduce true differences over time, thus reducing the precision of location estimates.

Modifications to components of our ARTS could enhance its performance; however, these modifications are associated with additional financial cost, reduced transmitter battery life and/or altered insect flight behaviour. Detection range of our ARTS is limited by the distance-power relationship. With our current receiver settings, locations can be estimated if the transmitter is between c. 25 to 150 m from a receiving station. Changing the receivers' gain could increase the distance at which signals are consistently detected or reduce the distance at which saturation occurs; additional calibration data would be required to describe the distance-power and angle-power relationships. Likewise, future transmitters that emit stronger signals, with low mass batteries, could also extend detection range and improve error estimates by increasing detection of power readings by receiving stations. Alternatively, additional receiving stations could be installed to extend the detectable range of the system; for example, rather than deploying four receiving stations to create a 250 m² detection area, nine receiving stations would create a 500 m² detection area. Additional receiving stations, antennae on receiving stations and/or antennae with more elements could improve tracking insects in flight, as suggested by Lenske and Nocera (2018) for tracking birds. Using a transmitter with a greater pulse rate could also aid in tracking insects in flight (e.g. see Lenske & Nocera, 2018) as well as decrease the error ellipse estimates.

To the best of our knowledge, this is the first ARTS designed to track insects (see Kissling et al., 2014 for a recent review of insect telemetry techniques). Using current, commercially available equipment, our findings likely represent the limit of existing ARTS technology to track non-migratory movement of insects. Although error estimates are large compared to ARTS using heavier, higher power transmitters for small mammals and birds, our system can estimate fine-scale locations within a 250 m² area at a frequency appropriate for our research questions. Estimating locations based on visual observations is not possible at these spatial and temporal scales. When combined with handheld radio telemetry to verify locations of tagged insects outside an ARTS' grid, this system provides a cost-effective means to estimate locations of insects at distances beyond human visual range. Our method with 0.22 g transmitters has potential to be adapted for use with other large insect species, small mammals and small birds.

ACKNOWLEDGEMENTS

Conversations with Anuj Sharma at Iowa State University's Institute for Transportation provided critical design ideas. Materials and logistical support were provided by Richard L. Hellmich, Keith G. Bidne and Craig A. Abel with the USDA-ARS CICGRU in Ames, IA. Thanks to our field site owners and managers for allowing access to their property: Mike Loan and Sarah Nolte at Blue Grass Enterprises, Adam Thomes and Ben Pease at Iowa State University's Turf Research Station at the Horticulture Farm, Justin Stensland at Stensland Sod, Warren Pierson at Iowa State University's Field Extension Education Laboratory (FEEL)

Farm, Kent Burns at the Iowa State University Dairy Farm and David Bruene at Iowa State University's Beef Teaching Farm. Field site recruitment was possible with guidance from Mark Honeyman and Adam Thomes. Special thanks to our technicians; data collection and troubleshooting this system could not have been accomplished without their dedication and positive attitudes: Cody Acevedo, Kevin Anderson, Cory Haggard, Signey Hilby, Jenna Nixt, Riley Nylin, Michael Roth, Samantha Shimota, Brooklyn Snyder, Kara Weber and Elke Windschitl. Kathleen Ray and Iowa State University's Statistic Consulting Group provided coding support. This work was supported, in part, by the Agriculture and Food Research Initiative Pollinator Health Program (Grant No. 2018-67013-27541) from the USDA National Institute of Food and the Agriculture and Iowa Agriculture and Home Economics Experiment Station. Project No. IOW03617 is supported by USDA/NIFA and State of Iowa funds. Any opinions, findings, conclusions or recommendations expressed in this publication are those of the authors and do not necessarily reflect the views of the U.S. Department of Agriculture.

AUTHORS' CONTRIBUTIONS

K.E.F., J.S.A. and S.P.B. conceived the ideas and designed the system; K.E.F. and S.P.B. collected the data; P.M.D. and G.H. developed the statistical methods and analysed the data; K.E.F. and P.M.D. led the manuscript writing. All authors contributed critically to manuscript drafts and gave final approval for publication.


PEER REVIEW

The peer review history for this article is available at <https://publons.com/publon/10.1111/2041-210X.13529>.

DATA AVAILABILITY STATEMENT

Data, metadata and R codes for this manuscript are publicly available through Github, Zenodo and Dryad: <https://github.com/kelseyefisher/locating-large-insects-using-automated-vhf-radio-telemetry-with-multi-antennae-array>; <https://zenodo.org/badge/latestdoi/260214221> (Fisher, 2020). Locating large insects using automated VHF radio telemetry with a multi-antennae array, Dryad Digital Repository <https://doi.org/10.5061/dryad.9kd51c5fn> (Fisher & Dixon, 2020)

ORCID

Kelsey Elizabeth Fisher  <https://orcid.org/0000-0002-9279-667X>
Phil M. Dixon  <https://orcid.org/0000-0002-1778-0686>

REFERENCES

- ARGOS System. (2020). Retrieved from <https://www.argos-system.org/>
- Balanis, C. A. (2016). *Antenna theory: Analysis and design* (4th ed.). Wiley.
- Barron, D. G., Brawn, J. D., & Weatherhead, P. J. (2010). Meta-analysis of transmitter effects on avian behavior and ecology. *Methods in Ecology and Evolution*, 1, 180–197. <https://doi.org/10.1111/j.2041-210X.2010.00013.x>
- Bates, D. M., & Watts, D. G. (2007). *Nonlinear regression analysis and its applications*. Wiley.
- Chan, Y., Tibbitts, T. L., Lok, T., Hassell, C. J., Peng, H., Ma, Z., Zhang, Z., & Piersma, T. (2019). Filling knowledge gaps in a threatened shorebird flyway through satellite tracking. *Journal of Applied Ecology*, 56, 2305–2315. <https://doi.org/10.1111/1365-2664.13474>
- Cochran, W., Swenson, G., & Pater, L. (2001). *Radio finding for wildlife research. Antenna applications symposium*: University of Illinois at Urbana-Champaign.
- Cochran, W. W., Warner, D. W., Tester, J. R., & Kuechle, V. B. (1965). Automatic radio-tracking system for monitoring animal movements. *BioScience*, 15, 98–100. <https://doi.org/10.2307/1293346>
- Crewe, T. L., Deakin, J. E., Beauchamp, A. T., & Morbey, Y. E. (2019). Detection range of songbirds using a stopover site by automated radio-telemetry. *Journal of Field Ornithology*, 90, 176–189. <https://doi.org/10.1111/jofo.12291>
- Drake, V. A., & Reynolds, D. R. (2012). *Radar entomology: Observing insect flight and migration*. CABI.
- Fernandez, P., Rodrigues, A., Obregon, R., de Haro, S., Jordano, D., & Fernandez-Haeger, J. (2016). Fine scale movement of the butterfly *Plebejus argus* in a heterogeneous natural landscape as revealed by GPS tracking. *Journal of Insect Behavior*, 29, 80–98.
- Fisher, K. E. (2020). Data from: Locating large insects using automated VHF radio telemetry with a multi-antennae array. *Zenodo*, Retrieved from <https://zenodo.org/badge/latestdoi/260214221>
- Fisher, K. E., Adelman, J. S., & Bradbury, S. P. (2020). Employing very high frequency (VHF) radio telemetry to recreate monarch butterfly flight paths. *Environmental Entomology*, 49(2), 312–323. <https://doi.org/10.1093/ee/nvaa019>
- Fisher, K. E., & Dixon, P. (2020). Data from: Locating large insects using automated VHF radio telemetry with a multi-antennae array. *Dryad Digital Repository*, <https://doi.org/10.5061/dryad.9kd51c5fn>
- Fornoff, F., Dechmann, D., & Wikelski, M. (2012). Observation of movement and activity via radio-telemetry reveals diurnal behavior of the neotropical katydid *Philophyllia ingens* (Orthoptera: Tettigoniidae). *Ecotropica*, 18, 27–34.
- Fownes, S., & Roland, J. (2002). Effects of meadow suitability on female behaviour in the alpine butterfly *Parnassius smintheus*. *Ecological Entomology*, 27, 457–466.
- Fris, H. T. (1946). A note on a simple transmission formula. *Proceedings of the IRE*, 34(5), 254–256. <https://doi.org/10.1109/JRPROC.1946.234568>
- Goldman, J., & Swenson, G. W. (1999). Radio wave propagation through woods. *IEEE Antennas and Propagation Magazine*, 41(5), 34–36. <https://doi.org/10.1109/74.801512>
- Grant, T. J., Parry, H. R., Zalucki, M. P., & Bradbury, S. P. (2018). Predicting monarch butterfly (*Danaus plexippus*) movement and egg-laying with a spatially-explicit agent-based model: The role of monarch perceptual range and spatial memory. *Ecological Modelling*, 374, 37–50. <https://doi.org/10.1016/j.ecolmodel.2018.02.011>
- Hagen, M., Wikelski, M., & Kissling, W. D. (2011). Space use of bumblebees (*Bombus* spp.) revealed by radio tracking. *PLoS ONE*, 6(5), e19997. <https://doi.org/10.1371/journal.pone.0019997>
- Hallworth, M. T., & Marra, P. P. (2016). Miniaturized GPS tags identify non-breeding territories of small breeding migratory songbird. *Scientific Reports*, 5, 11069. <https://doi.org/10.1038/srep11069>
- Johnson, R. A., & Wichern, D. W. (2002). *Applied multivariate statistical analysis* (5th ed.). Prentice Hall.
- Kallioniemi, E., Zannese, A., Tinker, J. E., & Franco, A. M. A. (2014). Inter- and intra-specific differences in butterfly behavior at boundaries. *Insect Conservation and Diversity*, 7, 232–240.
- Kays, R., Crofoot, M. C., Jetz, W., & Wikelski, M. (2015). Terrestrial animal tracking as an eye on life and planet. *Science*, 348(6240), aaa2478. <https://doi.org/10.1126/science.aaa2478>
- Kays, R., Tilak, S., Crofoot, M., Fountain, T., Obando, D., Ortega, A., Kuemmeth, F., Mandel, J., Swenson, G., Lambert, T., Hirsch, B., & Wikelski, M. (2011). Tracking animal location and activity with an automated radio telemetry system in a tropical rainforest. *The Computer Journal*, 5(12), 1931–1948. <https://doi.org/10.1093/comjnl/bxr072>

- Kissling, W. D., Pattemore, D. E., & Hagen, M. (2014). Challenges and prospects in the telemetry of insects. *Biological Reviews*, 89, 511–530. <https://doi.org/10.1111/brv.12065>
- Knight, S. M., Pitman, G. M., Flockhart, D. T. T., & Norris, D. R. (2019). Radio-tracking reveals how wind and temperature influence the pace of daytime insect migration. *Biology Letters*, 15, 20190327. <https://doi.org/10.1098/rsbl.2019.0327>
- Kuechle, V. B., & Kuechle, P. J. (2012). Radio telemetry in fresh water: The basics. In N. S. Adams, J. W. Beeman, & J. H. Eiler (Eds.), *Telemetry techniques: A user guide for fisheries research* (pp. 91–137). American Fisheries Society.
- Larkin, R. P., Raim, A., & Diehl, R. H. (1996). Performance of non-rotating direction-finder for automatic radio telemetry. *Journal of Field Ornithology*, 67, 59–71.
- Lenske, A. K., & Nocera, J. J. (2018). Field test of an automated radio-telemetry system: Tracking local space use of aerial insectivores. *Journal of Field Ornithology*, 89, 173–187. <https://doi.org/10.1111/jof.12254>
- Lenth, R. V. (1981). On finding the source of a signal. *Technometrics*, 23, 149–154. <https://doi.org/10.2307/1268030>
- Levett, S., & Walls, S. (2011). Tracking the elusive life of the Emperor Dragonfly *Anax imperator* Leach. *Journal of the British Dragonfly Society*, 27, 59–68.
- Liegeois, M., Tixier, P., & Beaudoin-Ollivier, L. (2016). Use of radio telemetry for studying flight movements of *Paysandisia archon* (Lepidoptera: Castniidae). *Journal of Insect Behavior*, 29(2), 199–213.
- Lotek Wireless Inc. (2020). Retrieved from <https://www.lotek.com/products/pinpoint-gps/>
- McMahon, L. A., Rachlow, J. L., Shipley, L. A., Forbey, J. S., Johnson, T. R., & Olsoy, P. J. (2017). Evaluation of micro-GPS receivers for tracking small-bodied mammals. *PLoS ONE*, 12(3), e0173185. <https://doi.org/10.1371/journal.pone.0173185>
- Merckx, T., Van Dyck, H., Karlsson, B., & Leimar, O. (2003). The evolution of movements and behaviour at boundaries in different landscapes: A common arena experiment with butterflies. *Proceedings of the Royal Society of London. Series B: Biological Sciences*, 270, 1815–1821.
- Motus Wildlife Tracking System. (2020). Retrieved from <https://motus.org>
- Murray, D. L., & Fuller, M. R. (2000). A critical review of the effects of marking on the biology of vertebrates. In F. T. Boitani L (Ed.), *Research techniques in animal ecology* (pp. 15–64). Columbia University Press.
- Nandintsetseg, D., Bracis, C., Olson, K. A., Bohning-Gaese, K., Calabrese, J. M., Chimeddorj, B., Fagan, W. F., Fleming, C. H., Heiner, M., Kaczensky, P., Leimgruber, P., Munkhnast, D., Stratmann, T., & Mueller, T. (2019). Challenges in the conservation of wide-ranging nomadic species. *Journal of Applied Ecology*, 56, 1916–1926. <https://doi.org/10.1111/1365-2664.13380>
- R Core Team. (2019). *R: A language and environment for statistical computing*. R Foundation for Statistical Computing. Retrieved from <https://www.R-project.org/>
- Schneider, C. W., Tautz, J., Grünwald, B., & Fuchs, S. (2012). RFID tracking of sublethal effects of two neonicotinoid insecticides on the foraging behavior of *Apis mellifera*. *PLoS ONE*, 7, e30023.
- Schultz, C. B. (1998). Dispersal behavior and its implications for reserve design in a rare Oregon butterfly. *Conservation Biology*, 12(2), 284–292.
- Schultz, C. B., & Crone, E. E. (2001). Edge-mediated dispersal behavior in a prairie butterfly. *Ecology*, 82(7), 1879–1892.
- Schultz, C. B., Franco, A. M., & Crone, E. E. (2012). Response of butterflies to structural and resource boundaries. *Journal of Animal Ecology*, 81, 724–734.
- Schultz, C. B., Pe'er, B. G., Damiani, C., Brown, L., & Crone, E. E. (2017). Does movement behaviour predict population densities? A test with 25 butterfly species. *Journal of Animal Ecology*, 86, 384–393.
- Semmens, B. X., Semmens, D. J., Thogmartin, W. E., Wiederholt, R., Lopez-Hoffman, L., Diffendorfer, J. E., Pleasants, J. M., Oberhauser, K. S., & Taylor, O. R. (2016). Quasi-extinction risk and population targets for the Eastern, migratory population of monarch butterflies (*Danaus plexippus*). *Scientific Reports*, 6, 23265. <https://doi.org/10.1038/srep23265>
- Skorka, P., Nowicki, P., Lenda, M., Witek, M., Sliwinski, E. B., Settele, J., & Woyciechowski, M. (2013). Different flight behaviour of the endangered scarce large blue butterfly *Phengaris teleius* (Lepidoptera: Lycaenidae) within and outside its habitat patches. *Landscape Ecology*, 28, 535–546.
- Srygley, R. B., & Kingsolver, J. G. (2000). Effects of weight loading on flight performance and survival of palatable Neotropical *Anartia fatima* butterflies. *Biological Journal of the Linnean Society*, 70, 707–725.
- Svensson, G. P., Sahlin, U., Brage, B., & Larsson, M. C. (2011). Should I stay or should I go? Modeling dispersal strategies in saproxylic insects based on pheromone capture and radio telemetry a case study on the threatened hermit beetle *Osmoderma eremita*. *Biodiversity and Conservation*, 20, 2883–2902.
- Taylor, P. D., Crewe, T. L., Mackenzie, S. A., Lepage, D., Aubry, Y., Crysler, Z., Finney, G., Francis, C. M., Guglielmo, C. G., Hamilton, D. J., Holberton, R. L., Loring, P. H., Mitchell, G. W., Norris, D. R., Paquet, J., Ronconi, R. A., Smetzer, J. R., Smith, P. A., Welch, L. J., & Woodworth, B. K. (2017). The MOTUS wildlife tracking system: A collaborative research network. *Avian Conservation and Ecology*, 12, 8. <https://doi.org/10.5751/ACE-00953-120108>
- Telemetry Solutions. (2017). Retrieved from <https://www.telemetrysolutions.com/wildlife-tracking-devices/gps-collars/micro-collars/>
- Thogmartin, W. E., Lopez-Hoffman, L., Rohweder, J., Diffendorfer, J., Drum, R., Semmens, S., Black, S., Caldwell, I., Cotter, D., Drobney, P., Jackson, L. L., Gale, M., Helmers, D., Hilburger, S., Howard, E., Oberhauser, K., Pleasants, J., Semmens, B., Taylor, O., ... Wiederholt, R. (2017). Restoring monarch butterfly habitat in the Midwestern US: 'all hands on deck'. *Environmental Research Letters*, 12, 074005. <https://doi.org/10.1088/1748-9326/aa7637>
- Tobias, J. A., & Pigot, A. L. (2019). Integrating behaviour and ecology into global biodiversity conservation strategies. *Philosophical Transactions of the Royal Society B: Biological Sciences*, 374, 20190012. <https://doi.org/10.1098/rstb.2019.0012>
- Turchin, P., Odendaal, F. J., & Rauscher, M. D. (1991). Quantifying insect movement in the field. *Environmental Entomology*, 20, 955–963.
- Wang, Z., Haug, Y., & Pierce, N. E. (2019). Radio telemetry helps record the dispersal patterns of birdwing butterflies in mountainous habitats: Golden Birdwing (*Troides aeacus*) as an example. *Journal of Insect Conservation*, 23, 729–738. <https://doi.org/10.1007/s10841-019-00167-5>
- Ward, M., Sperry, J., Weatherhead, P. (2013). Evaluation of automated radio telemetry for quantifying movements and home ranges of snakes. *Journal of Herpetology*, 47, 337–345. <https://doi.org/10.1670/12-018>
- White, G. C., & Garrott, R. A. (1990). *Analysis of wildlife radio-tracking data*. Academic Press.
- Wikelski, M., Moskowitz, D., Adelman, J. S., Cochran, J., Wilcove, D. S., & May, M. L. (2006). Simple rules guide dragonfly migration. *Biology Letters*, 2, 325–329. <https://doi.org/10.1098/rsbl.2006.0487>
- Wittmeyer, G., Northrup, J. M., & Bastille-Rousseau, G. (2019). Behavioural valuation of landscapes using movement data. *Philosophical Transactions of the Royal Society B: Biological Sciences*, 374, 20180046. <https://doi.org/10.1098/rstb.2018.0046>
- Wood, S. N. (2003). Thin-plate regression splines. *Journal of the Royal Statistical Society: Series B (Statistical Methodology)*, 65(1), 95–114. <https://doi.org/10.1111/1467-9868.00374>
- Wood, S. N. (2011). Fast stable restricted maximum likelihood and marginal likelihood estimation of semiparametric generalized linear models. *Journal of the Royal Statistical Society: Series B (Statistical Methodology)*, 73(1), 3–36. <https://doi.org/10.1111/j.1467-9868.2010.00749.x>
- Yagi-Uda.com. (2008). Retrieved from http://yagi-uda.com/three_elements_yagi-uda.php
- Zalucki, M. P., & Kitching, R. L. (1982). The analysis and description of movement in adult *Danaus plexippus* L. (Lepidoptera: Danainae). *Behaviour*, 80, 174–198.

Zalucki, M. P., Parry, H. R., & Zalucki, J. M. (2016). Movement and egg-laying in monarchs: To move or not to move, that is the equation. *Austral Ecology*, 41, 154–167. <https://doi.org/10.1111/aec.12285>

SUPPORTING INFORMATION

Additional supporting information may be found online in the Supporting Information section.

How to cite this article: Fisher KE, Dixon PM, Han G, Adelman JS, Bradbury SP. Locating large insects using automated VHF radio telemetry with a multi-antennae array. *Methods Ecol Evol.* 2021;12:494–506. <https://doi.org/10.1111/2041-210X.13529>